Cellular/Molecular

D1/D5 Dopamine Receptors and mGluR5 Jointly Enable Non-Hebbian Long-Term Potentiation at Sensory Synapses onto Lamina I Spinoparabrachial Neurons

Jie Li,[1] **Theodore J. Price,**[2] **and Mark L. Baccei**[1]

[1]Pain Research Center, Department of Anesthesiology, University of Cincinnati College of Medicine, Cincinnati, Ohio 45267, and [2]Center for Advanced Pain Studies, Department of Neuroscience, University of Texas at Dallas, Richardson, Texas 75080

Highly correlated firing of primary afferent inputs and lamina I projection neurons evokes synaptic long-term potentiation (LTP), a mechanism by which ascending nociceptive transmission can be amplified at the level of the spinal dorsal horn. However, the degree to which neuromodulatory signaling shapes the temporal window governing spike-timing-dependent plasticity (STDP) at sensory synapses onto projection neurons remains unclear. The present study demonstrates that activation of spinal D1/D5 dopamine receptors (D1/D5Rs) creates a highly permissive environment for the production of LTP in male and female adult mouse spinoparabrachial neurons by promoting non-Hebbian plasticity. Bath application of the mixed D1/D5R agonist SKF82958 unmasked LTP at STDP pairing intervals that normally fail to alter synaptic efficacy. Furthermore, during D1/D5R signaling, action potential discharge in projection neurons became dispensable for LTP generation, and primary afferent stimulation alone was sufficient to induce strengthening of sensory synapses. This non-Hebbian LTP was blocked by the D1/D5R antagonist SCH 39166 or genetic deletion of D5R, and required activation of mGluR5 and intracellular Ca^{2+} release but was independent of NMDAR activation. D1/D5R-enabled non-Hebbian plasticity was observed across multiple neuronal subpopulations in the superficial dorsal horn but was more prevalent in spinoparabrachial neurons than interneurons. Interestingly, the ability of neonatal tissue damage to promote non-Hebbian LTP in adult projection neurons was not observed in D5R knock-out mice. Collectively, these findings suggest that joint spinal D1/D5R and mGluR5 activation can allow unfettered potentiation of sensory synapses onto the output neurons responsible for conveying pain and itch information to the brain.

Key words: **dorsal horn; long-term potentiation; projection neuron; spike-timing-dependent plasticity; spinal cord; synaptic plasticity**

Significance Statement

Synaptic LTP in spinal projection neurons has been implicated in the generation of chronic pain. Under normal conditions, plasticity at sensory synapses onto adult mouse spinoparabrachial neurons follows strict Hebbian learning rules, requiring coincident presynaptic and postsynaptic firing. Here, we demonstrate that the activation of spinal D1/D5Rs promotes a switch from Hebbian to non-Hebbian LTP so that primary afferent stimulation alone is sufficient to evoke LTP in the absence of action potential discharge in projection neurons, which required joint activation of mGluR5 and intracellular Ca^{2+} release but not NMDARs. These results suggest that D1/D5Rs cooperate with mGluR5 receptors in the spinal dorsal horn to powerfully influence the amplification of ascending nociceptive transmission to the brain.

Introduction

Synaptic long-term potentiation (LTP) in the rodent dorsal horn can be evoked by peripheral nerve or tissue damage (Sandkühler and Liu, 1998; Zhang et al., 2004; Zhou et al., 2010) or by tetanic electrical stimulation protocols that evoke pain in rodents (Zhang et al., 2005; Hathway et al., 2009) and produce mechanical allodynia and secondary hyperalgesia in healthy human subjects (Klein et al., 2004; Hansen et al., 2007; Lang et al., 2007; Pfau et al., 2011). Furthermore, pharmacological agents that suppress LTP in the dorsal horn can dampen pain sensitivity in

Received Sep. 3, 2021; revised Oct. 21, 2021; accepted Nov. 12, 2021.

Author contributions: J.L., T.J.P., and M.L.B. designed research; J.L. performed research; J.L. and M.L.B. analyzed data; M.L.B. wrote the paper.

This work was supported by National Institutes of Health Grants NS080889 to M.L.B. and NS065926 to T.J.P. We thank Elizabeth Serafin for technical assistance on the project.

The authors declare no competing financial interests.

Correspondence should be addressed to Mark L. Baccei at mark.baccei@uc.edu.

https://doi.org/10.1523/JNEUROSCI.1793-21.2021

humans (Ruscheweyh et al., 2011), further supporting the potential clinical relevance of LTP. Emerging evidence suggests that synaptic plasticity occurs in a cell type-dependent manner in the superficial dorsal horn (SDH), as the electrical stimulation protocols that evoke LTP in projection neurons can evoke long-term depression (LTD) in GABAergic interneurons (H. Y. Kim et al., 2015; Li and Baccei, 2019). LTP at primary afferent synapses onto lamina I projection neurons likely plays a critical role in the amplification of ascending nociceptive transmission by the spinal cord under pathologic conditions (Ikeda et al., 2003, 2006; Drdla et al., 2009).

The tetanic stimulation protocols commonly used to examine LTP provide little information regarding the precise temporal rules governing the activity-dependent plasticity of sensory synapses onto projection neurons. Under normal conditions, plasticity at these synapses follows strict Hebbian learning rules. Namely, spike-timing-dependent LTP (t-LTP) is only evoked if the primary afferent input arrives during a brief time window (~10 ms) before the projection neuron fires but not if the order of activation is reversed (Li and Baccei, 2016). Nonetheless, the timing rules governing LTP at sensory synapses onto adult projection neurons can clearly be modified. As an example of such metaplasticity, early life tissue damage can unmask non-Hebbian LTP at these synapses as poorly correlated firing, or even paired activity occurring in the reverse order, can evoke LTP in neonatally incised mice (Li and Baccei, 2016).

Neuromodulators, including catecholamines, can profoundly regulate spike-timing-dependent plasticity (STDP) in the brain (Brzosko et al., 2019). For example, D1/D5 dopamine receptors (D1/D5Rs) in the hippocampus convert LTD to LTP so that LTP is observed regardless of the relative timing of presynaptic versus postsynaptic activity (Zhang et al., 2009). Dopamine is released in the spinal cord (Men and Matsui, 1994; Taepavarapruk et al., 2008; Benade et al., 2017), predominantly from fibers descending from the hypothalamic A11 nucleus that terminate throughout the gray matter (Björklund and Skagerberg, 1979; Qu et al., 2006; Koblinger et al., 2014). This can either dampen nociceptive signaling via activation of D2 receptors (Fleetwood-Walker et al., 1988; Wei et al., 2009; Taniguchi et al., 2011) or promote the sensitization of dorsal horn circuits via D1/D5Rs (J. Y. Kim et al., 2015; Megat et al., 2018). Unfortunately, nothing is known about how dopamine receptors shape STDP at primary afferent synapses onto spinal projection neurons. This prevents a complete understanding of the factors that govern the flow of nociceptive and pruriceptive information from the spinal cord to the brain.

In light of the documented ability of spinal D1/D5Rs to promote the transition from acute to chronic pain (J. Y. Kim et al., 2015; Megat et al., 2018), and given that D1/D5Rs facilitate LTP elsewhere in the CNS (Zhang et al., 2009), the present study tested the hypothesis that the timing rules governing STDP at primary afferent synapses onto lamina I projection neurons are modulated by D1/D5R-mediated signaling. The data clearly demonstrate that spinal D1/D5R activation strongly promotes non-Hebbian LTP at these synapses via mechanisms that depend on the joint activation of mGluR5 and downstream intracellular Ca^{2+} release. The data also suggest that D5R signaling contributes to the long-term metaplasticity of sensory synapses observed in the adult SDH following neonatal tissue injury. Collectively, these findings indicate that alterations in spinal dopaminergic tone could profoundly influence the gain of the SDH network as an amplifier of pain and itch signals.

Materials and Methods

Animals. All experiments were performed in accordance with animal welfare guidelines outlined by the Institutional Animal Care and Use Committee at the University of Cincinnati. Adult [postnatal day (P)63–80] male and female mice of the following genotypes were used in this study: (1) FVB-Tg(GadGFP)4570Swn mice, which express enhanced GFP (EGFP) in GABAergic neurons under the control of the *Gad67* promoter (The Jackson Laboratory; Oliva et al., 2000); (2) wild-type (WT; i.e., $Drd5^{+/+}$) C57BL/6J mice; and (3) $Drd5^{-/-}$ mice lacking D5R expression in which a neomycin resistance gene was ligated in reverse orientation into the unique *SfiI* site of the *Drd5* gene to disrupt the reading frame within the coding region (Holmes et al., 2001; Hollon et al., 2002).

Hindpaw surgical injury. $Drd5^{-/-}$ mice or wild-type controls were anesthetized with isoflurane (3–5%) at P3, and a small incision was made through the skin and underlying muscle of the plantar hindpaw as described previously (Brennan et al., 1996; Li et al., 2013). The skin was immediately closed with a 7–0 suture (Ethicon), and the wound fully healed in ≤2 weeks.

Retrograde labeling of spinoparabrachial neurons. Approximately 1 week before euthanasia, mice were anesthetized with a mixture of ketamine (90 mg/kg) and xylazine (10 mg/kg) given via intraperitoneal injection and secured in a stereotaxic apparatus. A single injection of FAST DiI oil (100–150 nl; 2.5 mg/ml) was administered into the parabrachial nucleus using a Hamilton micro-syringe (model #62RN; 2.5 µl volume) equipped with a 28 gauge removable needle. Based on an atlas by Paxinos and Franklin (2012), the following stereotaxic coordinates were used (in mm) relative to bregma: 4.8–5.0 caudal, 1.0–1.3 lateral, and 4.0–4.5 ventral.

Spinal cord slice preparation. Mice were deeply anesthetized with sodium pentobarbital (60 mg/kg) and perfused with ice-cold dissection solution consisting of the following (in mM): 250 sucrose, 2.5 KCl, 25 $NaHCO_3$, 1.0 NaH_2PO_4, 6 $MgCl_2$, 0.5 $CaCl_2$, and 25 glucose continuously bubbled with 95% O_2/5% CO_2. The lumbar spinal cord was isolated and immersed in low-melting-point agarose (3% in above solution; Life Technologies) and cooled on ice. Parasagittal slices (350–400 µm) with the L3–L4 dorsal roots attached (length 7–10 mm) were cut using a vibrating microtome (model #7000smz-2, Campden Instruments). Slices were incubated for 15–20 min in a recovery solution containing the following (in mM): 92 NMDG, 2.5 KCl, 1.2 NaH_2PO_4, 30 $NaHCO_3$, 20 HEPES, 25 glucose, 5 Na ascorbate, 2 thiourea, 3 Na pyruvate, 10 $MgSO_4$, and 0.5 $CaCl_2$ and then allowed to recover further in an oxygenated artificial CSF (aCSF) solution containing the following (in mM): 125 NaCl, 2.5 KCl, 25 $NaHCO_3$, 1.0 NaH_2PO_4, 1.0 $MgCl_2$, 2.0 $CaCl_2$, and 25 glucose for ≥1 h at room temperature.

Patch-clamp recordings. After recovery, slices (with attached dorsal roots) were transferred to a submersion-type recording chamber (RC-22, Warner Instruments) and mounted on the stage of an upright microscope (BX51WI; Olympus). Slices were then perfused at room temperature with oxygenated aCSF at a rate of 2–4 ml/min. Lamina I spinoparabrachial neurons were identified via DiI fluorescence, whereas GABAergic interneurons in laminae I–II were identified via EGFP fluorescence, and both were visualized for patch-clamp recording via infrared illumination.

Patch electrodes were constructed from thin-walled single-filamented borosilicate glass (1.5 mm outer diameter, World Precision Instruments) using a microelectrode puller (P-97, Sutter Instruments). Pipette resistances ranged from 4 to 6 MΩ, and seal resistances were >1 GΩ. Patch electrodes were filled with an intracellular solution containing the following (in mM): 130 K-gluconate, 10 KCl, 10 HEPES, 10 Na-phosphocreatine, 4 MgATP, and 0.3 Na_2-GTP, pH 7.2 (295–300 mOsm).

Whole-cell patch-clamp recordings were obtained from DiI-labeled projection neurons, *Gad67*-EGFP-labeled neurons, or adjacent non-GFP neurons in the L3/L4 dorsal horn using a Multiclamp 700B amplifier (Molecular Devices). EPSCs were evoked from a holding potential of −70 mV by electrical stimulation of the dorsal root (10 µA–1 mA, 100 µs) delivered via a suction electrode connected to a constant-current stimulator (Master-8). The threshold to evoke an EPSC was defined as the current intensity that evoked a measurable EPSC in ≥50% of the

trials. Monosynaptic EPSCs were defined by a stable onset latency (≤2 ms) and an absence of failures during repetitive stimulation, as described previously (Li and Baccei, 2016).

Induction of non-Hebbian LTP. Monosynaptic EPSCs were evoked in spinoparabrachial neurons, or dorsal horn interneurons, from a holding potential of −70 mV by stimulation of the attached dorsal root (every 15 s at an intensity of 1–1.2× threshold). Following the verification of a stable baseline EPSC amplitude for ≥5 min, the same primary afferent stimulus was paired with a postsynaptic action potential (AP) evoked by direct intracellular current injection (150–800 pA, 5 ms) at an interval ($\Delta t = t_{Pre} - t_{Post} = -50, +10$, or $+20$ ms) that normally fails to alter the efficacy of sensory synapses onto lamina I projection neurons (Li and Baccei, 2016). After administration of the pairing protocol (30 pairs of stimuli at 0.2 Hz), neurons were again voltage clamped (VC) at −70 mV, and the primary afferent-evoked EPSCs were recorded for ≥25 min to calculate a mean normalized change in EPSC amplitude (% baseline). In other experiments, presynaptic (i.e., primary afferent) or postsynaptic (projection neuron) stimulation was delivered alone (30 stimuli at 0.2 Hz). The above stimulation protocols were administered in the presence of vehicle or the mixed D1/D5R agonists SKF82958 (SKF) hydrobromide (100 nM or 10 μM; Tocris Bioscience) or A68930 HCl (2 μM; Tocris Bioscience), which were added to the bath solution in the absence or presence of the selective D1/D5R antagonist SCH 39166 (10 μM; Tocris Bioscience).

In a subset of experiments, the patch solution was supplemented with GTPγS (100 μM; Sigma-Aldrich) or GDPβS (2 mM; Sigma-Aldrich) to manipulate G-protein signaling in spinoparabrachial neurons. Alternatively, the intracellular solution was supplemented with BAPTA (30 mM) to chelate Ca^{2+} in projection neurons, ryanodine (RYAN; 100–200 μM) to prevent intracellular Ca^{2+} release from ryanodine-sensitive stores, MK801 (1 mM) to block postsynaptic NMDAR activity, or equivalent vehicle solutions as a control. An additional inhibitor of ryanodine-sensitive intracellular Ca^{2+} release, dantrolene (DANT; 30 μM), was applied via bath perfusion. The potential role of mGluR5 in the D1/D5R-enabled LTP was explored via the bath application of the selective mGluR5 antagonist MPEP (10 μM) or the selective mGluR5 agonist 2-Chloro-5-hydroxyphenylglycine (CHPG; 10 μM).

Membrane voltages were adjusted for liquid junction potentials (approximately −14 mV) calculated using JPCalc software (P. Barry, University of New South Wales, Sydney, Australia; modified for Molecular Devices). Currents were filtered at 4–6 kHz through a −3 dB, four-pole low-pass Bessel filter, digitally sampled at 20 kHz, and stored on a personal computer (Dell) using a commercially available data acquisition system (Digidata 1440A with pClamp 10.4 software, Molecular Devices).

Experimental design and statistical analysis. The following statistics were performed on measurements obtained from individual lamina I spinoparabrachial neurons rather than first averaging across all spinoparabrachial neurons sampled in the same mouse, given the known heterogeneity present within this population in terms of their soma size, dendritic morphology, expression of voltage-gated ion channels and neurotransmitter receptors, intrinsic firing properties, and their functional role in somatosensory coding (Cameron et al., 2015; Browne et al., 2021; Chisholm et al., 2021). As a result, in all figures, individual data points correspond to a single neuron.

The electrophysiological results shown in Figure 1*E* were collected from 17 neurons from 6 mice in the DMSO group (across three STDP pairing intervals) and 16 neurons from 13 mice in the SKF82958 group. Data were analyzed using two-way ANOVA with Drug and Pairing Interval as factors and Sidak's multiple-comparisons test. The effect of SKF82958 on baseline EPSC amplitude (Fig. 1*H*) was examined in a subset of experiments shown in Figure 1*E* (involving seven neurons from four mice), and data were analyzed with the Wilcoxon matched pairs test. Across two pairing protocols examined, the DMSO data displayed in Figure 2*E* and *F*, were obtained from 13 neurons from 6 wild-type mice and 13 neurons from 5 D5R knock-out mice, whereas the SKF89258 results were collected from 17 neurons in 8 wild-type mice and 15 neurons from 5 D5R knock-out mice. These data were analyzed by three-way ANOVA with Drug, Pairing Interval, and Genotype as factors and Sidak's multiple-comparisons test.

For the study exploring the ability of D5R knock-out to modulate the effects of neonatal injury on STDP (Fig. 3), data in the Naive group encompassed recordings from 17 neurons from 8 wild-type mice and 20 neurons from 9 D5R knock-out mice (across two pairing intervals), whereas the P3 incision dataset reflected results from 12 neurons from 6 wild-type mice and 14 neurons from 6 D5R knock-out mice. Data were analyzed via three-way ANOVA with Injury, Genotype, and Pairing Interval as factors and Sidak's multiple-comparisons test. The experiments illustrated in Figure 4*A* involved the following group sizes: SKF Only: eight neurons from five mice, vehicle (VEH) + Pre only: 17 neurons from six mice, SKF + Pre only [projection neurons (PN) in current clamp (CC)]: six neurons from four mice; SKF + Pre only (PN in VC): 17 neurons from 10 mice, SKF + Pre only + SCH 39166: nine neurons from four mice, and SKF + Post only: six neurons from four mice. Data in Figure 4*A* were analyzed using one-way ANOVA with Dunnett's multiple-comparisons test. Meanwhile, the studies investigating potential sex differences in non-Hebbian plasticity (Fig. 4*B*) involved recording from eight neurons in three male mice and nine neurons from three female mice in the DMSO group, whereas the SKF82958 group involved nine neurons from three male mice and eight neurons from seven female mice. These data were analyzed using two-way ANOVA with Sex and Drug as factors and Sidak's multiple-comparisons test. Finally, the data shown in Figure 4*D* reflected the sampling of 17 neurons from 10 wild-type mice and 14 neurons from 9 D5R knock-out mice and were analyzed via repeated measures (RM) two-way ANOVA with Stimulation and Genotype as factors and Sidak's multiple-comparisons test.

The experimental groups displayed in Figure 5 involved sampling (from left to right) seven neurons from five D5R knock-out mice, six neurons from three D5R knock-out mice, six neurons from five D5R knock-out mice, and eight neurons from four wild-type mice. These results were analyzed with one-way ANOVA and Tukey's multiple-comparisons test. For the studies illustrated in Figure 6*C*, seven neurons were recorded from two mice in the Control (vehicle) group, six neurons from three mice were treated with intracellular MK801, and data were analyzed with the Mann–Whitney test. The dataset shown in Figure 6*D* involved the following group sizes: VEH: eight neurons from seven mice, MK801: eight neurons from four mice, BAPTA: 10 neurons from six mice, and MPEP: seven neurons from four mice, and the results were analyzed using one-way ANOVA and Dunnett's multiple-comparisons test. The data from Figure 6*E* originated from five neurons from two mice in the VEH group, six neurons from three mice in the DANT group, and seven neurons from three mice in the RYAN group and were compared across groups using one-way ANOVA and Dunnett's multiple-comparisons test. Meanwhile, the data in Figure 6*F* were analyzed with one-way ANOVA and Tukey's post test and included six neurons from three mice in the SKF only group, six neurons from five mice in the CHPG only group, and eight neurons from five mice in the SKF + CHPG group. Finally, the results shown in Figure 7 originated from the sampling of 10 PNs from 6 mice in addition to 16 *Gad67*-EGFP neurons and 15 non-GFP neurons from 11 mice. In Figure 7*A*, neurons were classified as exhibiting LTP or LTD if the EPSC amplitudes at baseline (in response to 20 consecutive stimuli delivered to the dorsal root) were found to be significantly different from the EPSC amplitudes recorded at $t = 20–25$ min after administration of the STDP pairing protocol using a paired t test. Data in Figure 7*B* were analyzed via the Kruskal–Wallis test with Dunnett's multiple-comparisons test.

Results

Spinal D1/D5R activation facilitates spike-timing-dependent LTP at primary afferent synapses onto lamina I projection neurons

To begin determining the extent to which D1/D5R signaling modifies the timing rules governing STDP at sensory synapses onto lamina I spinoparabrachial neurons, primary afferent stimulation was paired with AP firing in projection neurons (Fig. 1*A*) at intervals that we have previously shown to produce no changes in synaptic efficacy (Li and Baccei, 2016) either in the

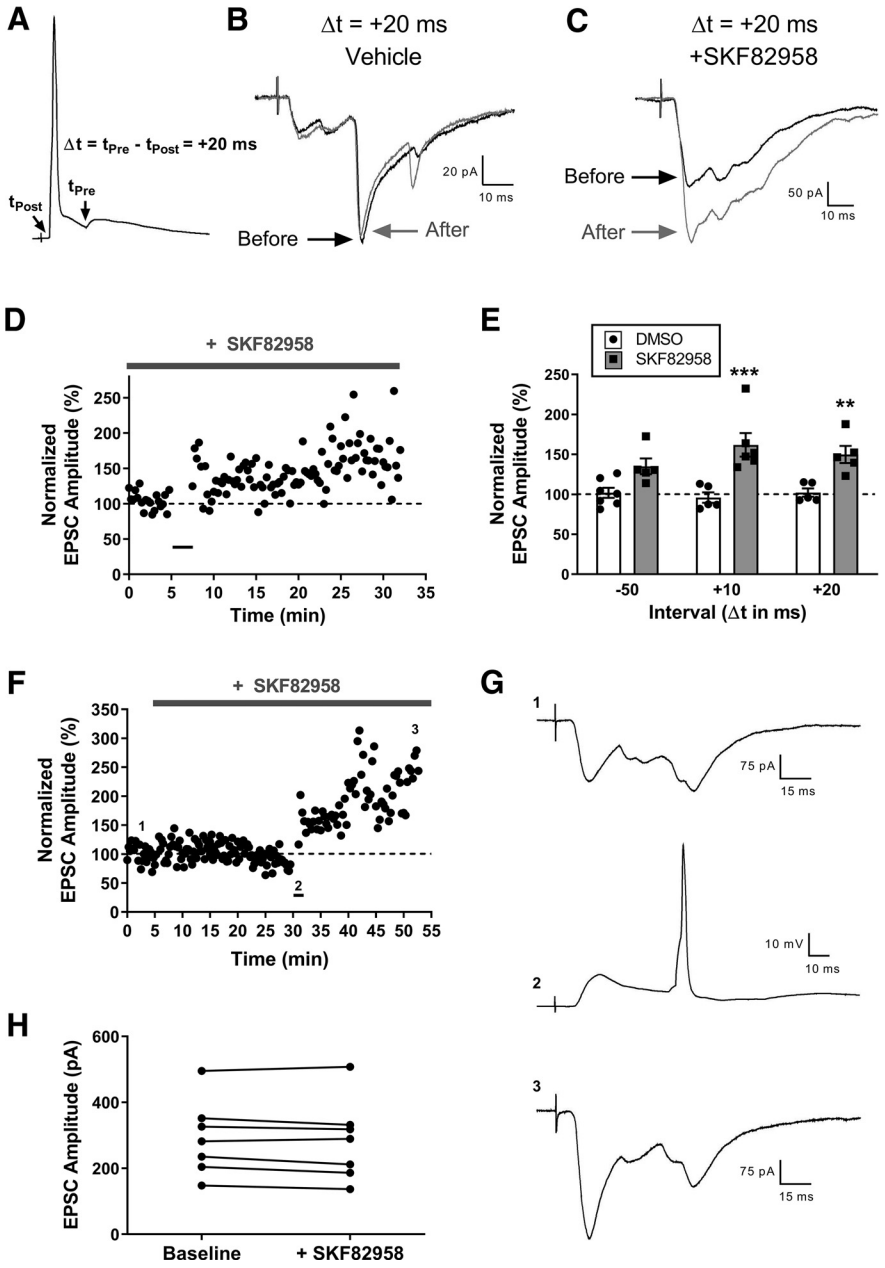

Figure 1. D1/D5 dopamine receptor signaling relaxes the timing rules governing LTP at sensory synapses onto lamina I spinoparabrachial neurons. ***A***, Example of STDP pairing protocol in which an action potential was induced in the projection neuron 20 ms before the onset of a monosynaptic EPSP evoked by stimulating the attached dorsal root. ***B***, Representative EPSCs evoked by primary afferent stimulation before (black) and after (gray) administration of the chosen pairing protocol ($\Delta t = +20$ ms; 30 pairs at 0.2 Hz) in the presence of the vehicle solution (0.01% DMSO). ***C***, A different projection neuron exhibited a clear increase in EPSC amplitude when the same pairing protocol was combined with bath application of the mixed D1/D5R agonist SKF82958. ***D***, Representative plot of EPSC amplitude, normalized to the mean amplitude before administration of the pairing protocol (black bar), as a function of time showing that the combined presence of SKF82958 and a normally ineffective pairing protocol ($\Delta t = +20$ ms) evoked LTP at primary afferent synapses onto lamina I spinoparabrachial neurons sampled from *Gad67*-EGFP mice. ***E***, Perfusion of SKF82958 enabled LTP at pairing intervals that normally fail to alter synaptic strength (Drug: $F_{(1,27)} = 38.12$, $p < 0.0001$, two-way ANOVA; $^{**}p = 0.007$, $^{***}p = 0.0001$ compared with DMSO control, Sidak's multiple-comparisons test). ***F***, Representative plot of normalized EPSC amplitude versus time demonstrating that the continued application of SKF82958 alone fails to modulate EPSC amplitude, which is subsequently increased following the administration of a normally ineffective pairing protocol ($\Delta t = -50$ ms). ***G***, Representative synaptic responses at different time points (1–3) for the same neuron illustrated in ***F*** (1, baseline EPSC; 2, primary afferent-evoked EPSP paired with postsynaptic action potential; 3, EPSC after administration of pairing protocol). ***H***, Perfusion with SKF82958 alone (i.e., in the absence of the pairing protocol) did not modify the amplitude of monosynaptic primary afferent-evoked EPSCs ($W = 7$, $p = 0.156$, Wilcoxon matched pairs test). ***B***, ***C***, ***G***, The displayed traces reflect the average of 20 consecutive responses.

presence of the mixed D1/D5R agonist SKF82958 (10 μM) or DMSO as a vehicle control. In the presence of the vehicle solution, paired presynaptic and postsynaptic stimulation at intervals ($\Delta t = t_{Pre} - t_{Post}$) of −50, +10, or +20 ms failed to alter the efficacy of primary afferent synapses onto spinoparabrachial neurons (Fig. 1*B*,*E*). Strikingly, the delivery of the same STDP pairing protocols in the presence of SKF82958 evoked clear LTP (Drug: $F_{(1,27)} = 38.12$, $p < 0.0001$, two-way ANOVA; Fig. 1*C*–*E*). To exclude the possibility that SKF82958 caused a delayed increase in EPSC amplitude independently of the pairing protocol, primary afferent stimulation at the baseline frequency (0.067 Hz) was extended for 30 min in the continued presence of SKF82958 before the administration of the STDP pairing protocol (Fig. 1*F*). Importantly, the bath application of SKF82958 alone did not alter the amplitude of primary afferent-evoked EPSCs in spinoparabrachial neurons ($W = 7$, $p = 0.156$, Wilcoxon matched pairs test; Fig. 1*H*), and LTP was only induced on the subsequent administration of the pairing protocol (Fig. 1*F*,*G*). Collectively, these results suggest that activation of spinal D1/D5Rs alone does not modulate the efficacy of sensory synapses onto ascending projection neurons but nonetheless significantly relaxes the timing rules governing spike-timing-dependent LTP within these key output neurons of the dorsal horn network.

Because SKF82958 cannot distinguish between D1Rs and D5Rs, the dopamine receptor subtypes that facilitate LTP at primary afferent synapses onto lamina I spinoparabrachial neurons remained unclear. To address a potential role of D5Rs, we repeated a subset of the above experiments using mice with a global deletion of the *Drd5* gene encoding the D5R (Holmes et al., 2001; Hollon et al., 2002). First, as seen when recording from lamina I spinoparabrachial neurons from *Gad67*-EGFP mice on the FVB genetic background (Fig. 1), the bath administration of SKF82958 promoted LTP at normally ineffective pairing intervals in lamina I spinoparabrachial neurons sampled from wild-type C57BL/6 mice (Fig. 2*E*). More importantly, the ability of SKF82958 to facilitate LTP was absent across the population of spinoparabrachial neurons sampled from D5R knock-out mice (Drug × Genotype Interaction: $F_{(1,50)} = 6.636$, $p = 0.013$, three-way ANOVA; Fig. 2*A*–*E*). Overall, these results identify a key role for spinal D5Rs in the production of non-Hebbian LTP at sensory synapses in the presence of SKF82958.

D5R knock-out prevents the facilitation of t-LTP at sensory synapses onto adult spinoparabrachial neurons following neonatal tissue damage

Our previous studies clearly showed that neonatal hindpaw incision significantly widened the temporal window governing t-LTP at primary afferent synapses onto adult lamina I spinoparabrachial neurons sampled from mice on the FVB genetic background (Li and Baccei, 2016). Similarly, here we demonstrate that unilateral hindpaw incision at P3 in wild-type C57BL/6 mice unmasks t-LTP at mature sensory synapses at pairing intervals that fail to consistently enhance synaptic efficacy in naive littermate controls (Fig. 3), thereby confirming that the ability of early life trauma to evoke synaptic metaplasticity in the mature SDH extends across multiple genetic strains of mice. However, in adult C57BL/6 mice lacking D5R expression, there was no significant difference in the observed synaptic plasticity between the naive and neonatally incised littermates at either pairing interval examined (Injury × Genotype Interaction: $F_{(1,55)} = 9.339$, $p = 0.004$, three-way ANOVA; Fig. 3). These data suggest that D5R-mediated signaling is important for the persistent effects of early life tissue damage on the properties of activity-dependent plasticity at primary afferent inputs onto mature spinoparabrachial neurons.

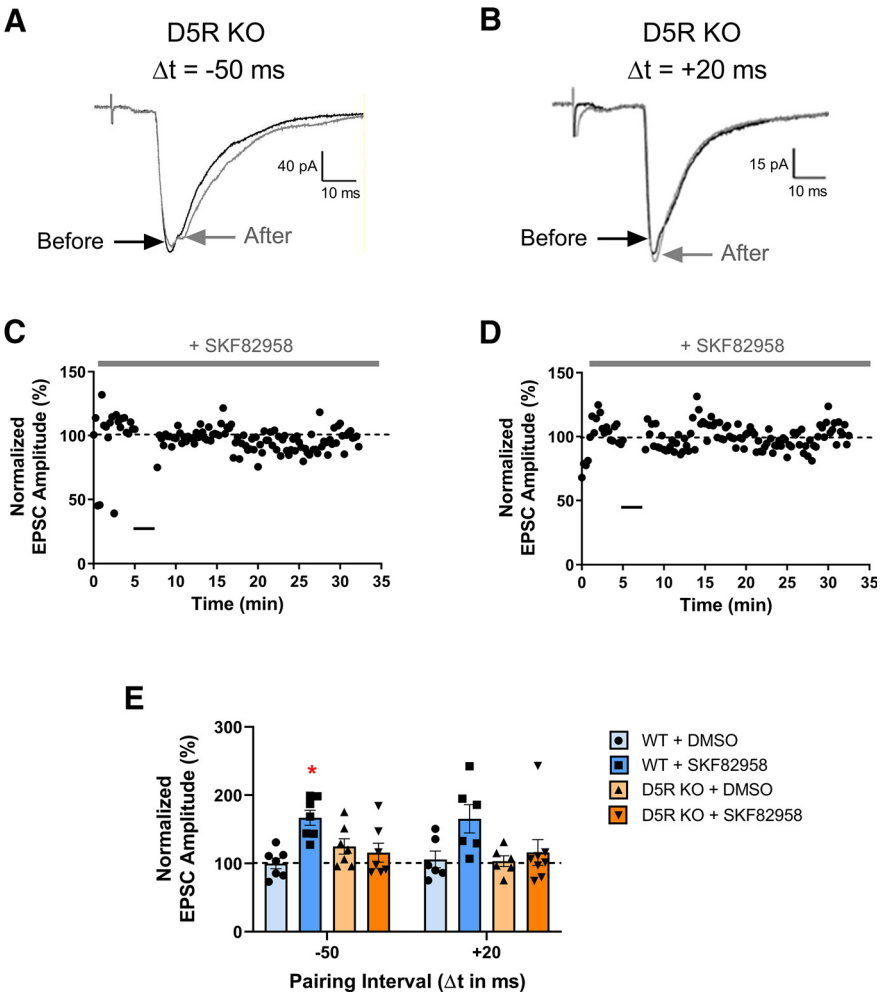

Figure 2. D5R activation is required for non-Hebbian LTP enabled by SKF82958. ***A***, ***B***, Representative primary afferent-evoked EPSCs in lamina I spinoparabrachial neurons from D5R KO mice before (black) and after (gray) administration of STDP pairing protocols at $\Delta t = -50$ ms (***A***) or $\Delta t = +20$ ms (***B***) in the presence of the D1/D5R agonist SKF82958. ***C***, ***D***, Representative plots of normalized EPSC amplitude as a function of time for the corresponding neurons displayed in ***A*** and ***B***, showing that the joint application of SKF82958 and the indicated pairing protocol fail to induce LTP in projection neurons from D5R KO mice. ***E***, Although SKF82958 enabled LTP in response to normally ineffective pairing intervals in WT projection neurons (Drug: $F_{(1,50)} = 7.647$, $p = 0.008$; Pairing Interval: $F_{(1,50)} = 0.107$, $p = 0.745$, three-way ANOVA; $^*p < 0.05$, Sidak's multiple-comparisons test compared with corresponding DMSO control), this plasticity was abolished by the genetic deletion of D5R (Drug × Genotype Interaction: $F_{(1,50)} = 6.636$, $p = 0.013$, three-way ANOVA).

AP discharge in spinoparabrachial neurons becomes dispensable for the potentiation of sensory synapses in the presence of D1/D5R activation

One mechanism by which D1/D5R signaling could facilitate LTP at these synapses is by removing the strict requirement that the presynaptic (i.e., primary afferent) input and postsynaptic neuron (i.e., projection neuron) both fire within a certain time window (Li and Baccei, 2016). This possibility was investigated by examining the effects of presynaptic stimulation alone (i.e., dorsal root stimulation at 0.2 Hz, 30 trials), or postsynaptic stimulation alone (i.e., 30 APs elicited in the projection neuron via intracellular current injections at 0.2 Hz) on the amplitude of monosynaptic primary afferent-evoked EPSCs in lamina I spinoparabrachial neurons from naive mice. As expected based on our prior findings (Li and Baccei, 2016), primary afferent stimulation alone in the presence of a control vehicle solution did not significantly alter EPSC amplitude in projection neurons (VEH + Pre only: 99.5 ± 4.7% of baseline; Fig. 4*A*, green). However, in the presence of the selective D1/D5R agonist SKF82958, dorsal root stimulation alone was sufficient to evoke LTP at primary afferent synapses onto spinoparabrachial neurons, regardless of whether the projection neuron was VC at −70 mV throughout the experiment (SKF + Pre only (PN in VC): 143.6 ± 7.1% of baseline; $F_{(5,57)} = 14.59$, $p < 0.0001$, one-way ANOVA; $p < 0.0001$ compared with SKF only, Dunnett's multiple-comparisons test; Fig. 4*A*, blue) or instead allowed to depolarize under CC conditions during the dorsal root stimulation (SKF + Pre only (PN in CC): 138.8 ± 9.3% of baseline; $p = 0.0007$ compared with SKF only; Fig. 4A, yellow). This non-Hebbian LTP was abolished when the selective D1/D5R antagonist SCH 39166 was coadministered with the SKF82958 and presynaptic stimulation (Fig. 4*A*, orange). Importantly, no change in synaptic strength was seen if the SKF82958 application was paired with the direct induction of AP discharge in the spinoparabrachial neuron (SKF + Post only: 102.3 ± 5.2% of baseline; Fig. 4*A*, purple).

Given that spinal D1Rs and D5Rs can regulate spinal nociceptive processing in a sex-dependent manner (Megat et al., 2018), we next sought to determine whether the non-Hebbian LTP unleashed by D1/D5R activation occurred in projection neurons from both male and female mice. The combination of SKF82958 application (10 μM) and primary afferent stimulation significantly enhanced EPSC amplitude (Drug: $F_{(1,30)} = 25.95$, $p < 0.0001$, two-way ANOVA) regardless of sex (Drug × Sex Interaction: $F_{(1,30)} = 0.558$, $p = 0.461$, two-way ANOVA; Fig. 4*B*).

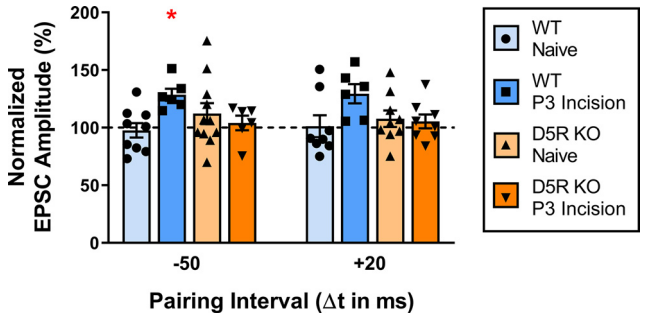

Figure 3. Neonatal surgical injury fails to modulate t-LTP in adult projection neurons from D5R knock-out mice. In adult lamina I spinoparabrachial neurons from WT mice, unilateral hindpaw incision at P3 facilitated t-LTP at STDP pairing intervals that produced no LTP in naive littermate controls (Injury: $F_{(1,55)} = 4.559$, $p = 0.037$; Pairing Interval: $F_{(1,55)} = 0.004$, $p = 0.95$, three-way ANOVA; $^*p < 0.05$, Sidak's multiple-comparisons test compared with corresponding naive control). In contrast, in projection neurons sampled from D5R KO mice, there were no observed differences in synaptic plasticity between P3-incised and naive littermates at either pairing interval examined (Injury × Genotype Interaction: $F_{(1,55)} = 9.339$, $p = 0.004$, three-way ANOVA).

A lower concentration of SKF82958 (100 nM) failed to induce LTP when combined with presynaptic stimulation (108.0 ± 6.6% of baseline; $n = 7$, $p > 0.05$ compared with DMSO control, one-way ANOVA; data not shown). Meanwhile the bath application of A68930, another selective D1/D5R agonist that is structurally dissimilar to SKF82958, was also able to potentiate primary afferent synapses onto spinoparabrachial neurons when combined with presynaptic stimulation (138.0 ± 9.9% of baseline; $n = 7$; Fig. 4*C*) despite failing to alter EPSC amplitude on its own. To further confirm that the non-Hebbian LTP witnessed in the presence of SKF82958 resulted from activation of D1/D5Rs, dorsal root stimulation was jointly applied with bath perfusion of SKF82958 (10 μM) in lamina I spinoparabrachial neurons from D5R knock-out mice. The combination of primary afferent stimulation and SKF82958 failed to evoke LTP at sensory synapses onto projection neurons from D5R knock-out mice (Genotype × Stimulation Interaction: $F_{(1,29)} = 15.98$, $p = 0.0004$, RM two-way ANOVA; Fig. 4*D*). Notably, this suppression of non-Hebbian LTP was similar in projection neurons from male (112.9 ± 9.4% of baseline, $n = 7$) and female (108.5 ± 8.1% of baseline, $n = 8$) D5R knock-out mice (data not shown). Collectively, the above results strongly indicate that spinal D1/D5R activation enables non-Hebbian LTP at primary afferent synapses onto spinoparabrachial neurons by removing the need for postsynaptic firing.

In light of the known ability of D1/D5Rs to activate G_s-mediated signaling (Boyd and Mailman, 2012), we next sought to confirm that postsynaptic G-protein activity was required to evoke non-Hebbian LTP at these synapses. Although the genetic deletion of D5R prevented the SKF82958-evoked LTP across the population of spinoparabrachial neurons as mentioned above (Fig. 5*A*, white), the addition of GTPγS to the intracellular solution to stimulate G-protein signaling downstream of D1/D5R activation restored the LTP evoked by primary afferent stimulation alone ($F_{(3,23)} = 5.2$, $p = 0.0069$, one-way ANOVA; $p = 0.049$ compared with SKF + Pre only in D5R KO, Tukey's multiple-comparisons test; Fig. 5, light gray). Importantly, the intracellular delivery of GTPγS to projection neurons was not itself sufficient to evoke LTP in the D5R knock-out mice (Fig. 5, medium gray), thereby demonstrating that a combination of primary afferent input and postsynaptic G-protein activity is essential to generate non-Hebbian plasticity at these synapses. Finally, in spinoparabrachial neurons from wild-type (WT) mice, the inclusion of GDPβS in the intracellular solution to block postsynaptic G-protein activity prevented the synaptic strengthening normally evoked by coupling dorsal root stimulation with bath application of SKF82958 (Fig. 5, dark gray). These findings further support the notion that sensory input and G-protein signaling cooperate to strengthen primary afferent synapses onto ascending projection neurons in the absence of correlated presynaptic and postsynaptic firing.

D1/D5R-enabled non-Hebbian LTP requires joint activation of mGluR5 and intracellular Ca^{2+} release

Spike-timing-dependent LTP in projection neurons under naive conditions critically depends on NMDARs (Li and Baccei, 2016). To elucidate the extent to which NMDARs expressed by lamina I spinoparabrachial neurons drives the non-Hebbian plasticity observed in the presence of D1/D5R activation, the selective NMDAR antagonist MK801 was added to the patch solution to selectively block postsynaptic NMDARs. Intracellular MK801 (1 mM) effectively blocked NMDARs within the sampled projection neurons as it largely prevented the enhancement of primary afferent-evoked EPSCs following perfusion with an external bath solution containing zero Mg^{2+} ($U = 1$; $p = 0.002$ compared with intracellular vehicle control; Mann–Whitney test; Fig. 6*A–C*). In contrast, intracellular MK801 failed to prevent the LTP evoked by primary afferent stimulation (i.e., Pre only) in the presence of SKF82958 ($p > 0.999$, Dunnett's multiple-comparisons test; Fig. 6*D*, light gray). Nonetheless, the non-Hebbian plasticity enabled by D1/D5R signaling clearly required an elevation in intracellular Ca^{2+} within projection neurons as the addition of BAPTA to the patch solution blocked the LTP ($F_{(3,29)} = 4.481$, $p = 0.011$, one-way ANOVA; $p = 0.033$ compared with Vehicle, Dunnett's post test; Fig. 6*D*, medium gray). Collectively, these results suggest that NMDARs are not the key source of intracellular Ca^{2+} driving the activity-dependent strengthening of primary afferent synapses in the presence of D1/D5R signaling.

Group I mGluRs (mGluR1/5) and downstream intracellular Ca^{2+} release can drive the generation of Hebbian spike-timing-dependent LTP in rat substantia gelatinosa neurons following highly correlated presynaptic and postsynaptic firing ($\Delta t = -5$ ms; Jung et al., 2006). To determine whether mGluR5 plays a role in enabling non-Hebbian LTP within projection neurons in the presence of D1/D5R activity, the selective mGluR5 antagonist MPEP was bath applied to the slice before the combined administration of primary afferent stimulation (i.e., Pre only) and SKF82958. Importantly, MPEP prevented the generation of non-Hebbian LTP under these conditions ($p = 0.042$ compared with vehicle, Dunnett's post test; Fig. 6*D*, dark gray). In addition, non-Hebbian LTP was not seen when intracellular Ca^{2+} release from ryanodine-sensitive stores was disrupted via the bath administration of the ryanodine receptor (RyR) antagonist dantrolene ($F_{(2,15)} = 5.613$, $p = 0.015$, one-way ANOVA; $p = 0.02$ compared with vehicle, Dunnett's multiple-comparisons test; Fig. 6*E*, light gray). To explore the importance of postsynaptic intracellular Ca^{2+} release within spinoparabrachial neurons for the non-Hebbian LTP seen during D1/D5R activation, parallel studies involved the inclusion of the RyR antagonist ryanodine in the patch solution. Internal delivery of ryanodine prevented the LTP normally evoked by joint dorsal root stimulation and SKF82958 application ($p = 0.016$ compared with vehicle, Dunnett's post test; Fig. 6*E*, dark gray).

The above data are consistent with the possibility that the activation of mGluR5 receptors by glutamate released from

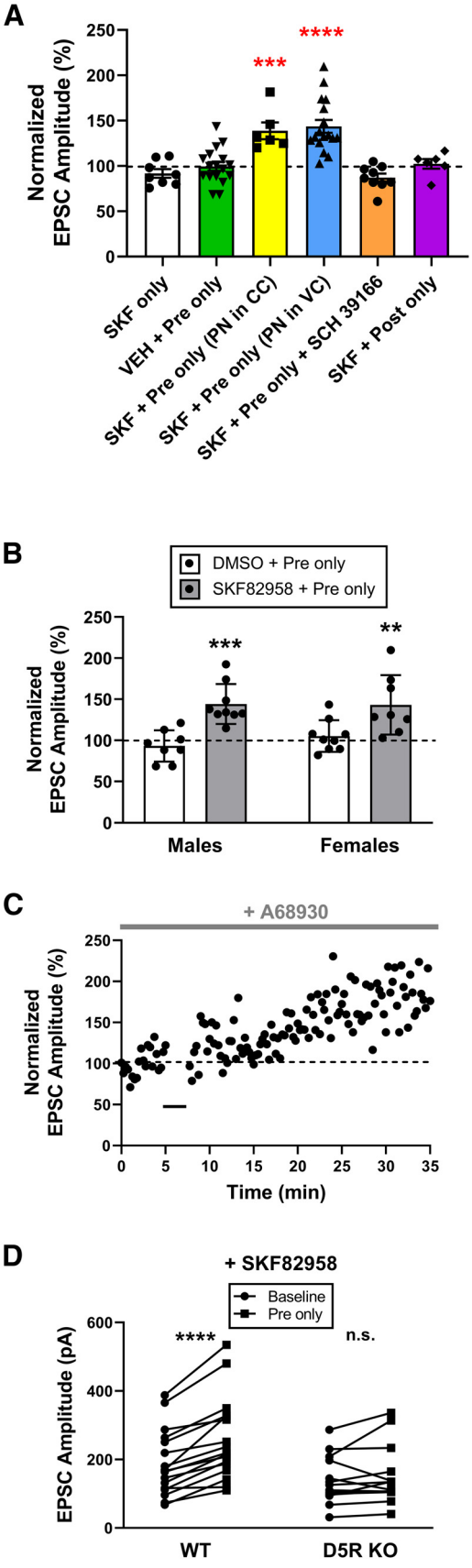

Figure 4. D1/D5R activation enhances LTP at sensory synapses onto spinal projection neurons in both sexes by removing the need for postsynaptic firing. ***A***, Plot of normalized EPSC amplitude following administration of SKF alone (white), DMSO VEH solution combined with primary afferent stimulation only (i.e., Pre only; green), SKF perfusion combined with primary afferent stimulation only (i.e., no postsynaptic action potential) delivered with the PN in the CC mode (yellow) or voltage clamped at −70 mV during dorsal root stimulation (blue), SKF perfusion combined with primary afferent stimulation only in the presence of the selective D1/D5R antagonist SCH 39166 (orange), or SKF perfusion combined with induced postsynaptic action potential discharge in the projection neuron (Post only; purple). For the groups in white, green, and orange, projection neurons were voltage clamped at −70 mV throughout the experiment. In the presence of D1/D5R signaling, primary afferent input alone was sufficient to induce LTP regardless of the level of postsynaptic depolarization ($F_{(5,57)} = 14.59$, $p < 0.0001$, one-way ANOVA; ***$p = 0.0007$, ****$p < 0.0001$ compared with SKF only, Dunnett's post test). ***B***, Joint primary afferent stimulation and D1/D5R activation evoked LTP in projection neurons from both males and females (Drug × Sex Interaction: $F_{(1,30)} = 0.558$, $p = 0.461$, two-way ANOVA; **$p = 0.009$, ***$p = 0.0005$ compared with DMSO, Sidak's multiple-comparisons test). ***C***, Representative plot of normalized EPSC amplitude as a function of time showing that the bath application of the D1/D5R agonist A68930 induced synaptic potentiation when paired with dorsal root stimulation (black bar). ***D***, SKF82958 combined with primary afferent stimulation evokes LTP in spinoparabrachial neurons from WT mice but not in spinoparabrachial neurons from D5R knock-out mice (Genotype × Stimulation Interaction: $F_{(1,29)} = 15.98$, $p = 0.0004$, RM two-way ANOVA; ****$p < 0.0001$, Sidak's post test); n.s., Not significant.

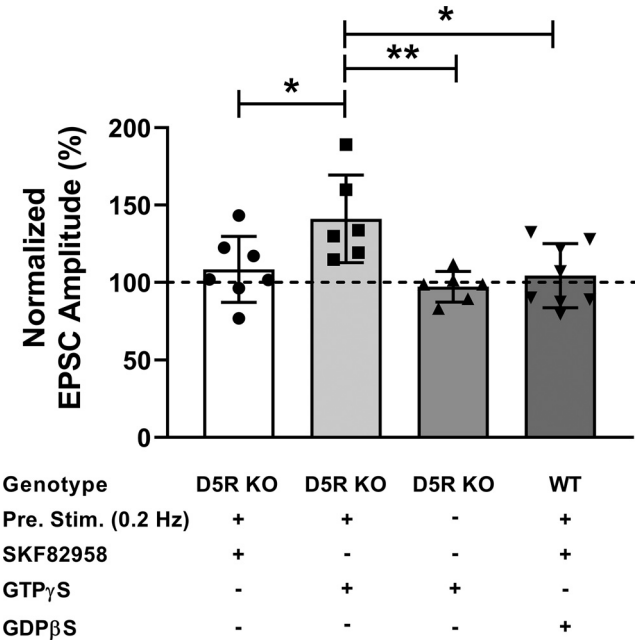

Figure 5. Role of postsynaptic G-protein signaling in D1/D5R-mediated non-Hebbian LTP in spinal projection neurons. Although genetic deletion of D5R (D5R KO) prevented the induction of LTP following joint application of SKF82958 and dorsal root stimulation (white), the activation of postsynaptic G-protein signaling via the addition of GTPγS into the patch solution was sufficient to drive non-Hebbian LTP in presence of primary afferent input (light gray) but did not alter synaptic efficacy on its own (medium gray). Meanwhile, the inclusion of GDPβS in the patch solution abolished the LTP normally produced by combined SKF82958 and dorsal root stimulation in projection neurons from WT mice (dark gray), further supporting the importance of postsynaptic G-protein signaling for the non-Hebbian plasticity enabled by D1/D5R activation ($F_{(3,23)} = 5.2$, $p = 0.0069$, one-way ANOVA; *$p < 0.05$, **$p < 0.01$, Tukey's multiple-comparisons test).

sensory neurons is essential for non-Hebbian LTP under conditions of D1/D5R activity, which could explain why SKF82958 application alone is incapable of potentiating primary afferent synapses onto lamina I spinoparabrachial neurons (Figs. 1*H*, 4*A*). To examine whether mGluR5 signaling is sufficient to evoke non-Hebbian LTP in the presence of D1/D5R activation, projection neurons (under voltage clamp at −70 mV) were perfused with SKF82958 alone, the selective mGluR5 agonist CHPG alone, or both SKF82958 and CHPG in the absence of dorsal root

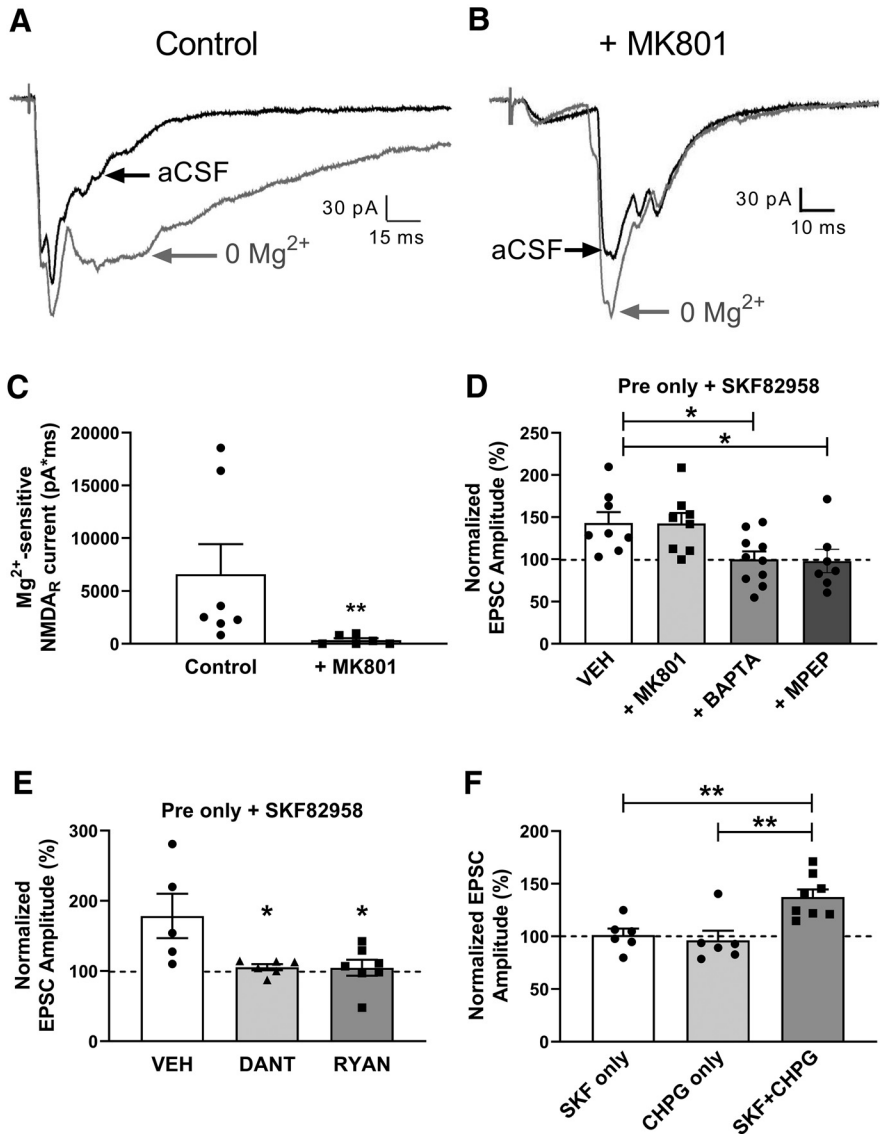

Figure 6. mGluR5 activation and intracellular Ca^{2+} release, but not NMDARs, are essential for D1/D5R-driven non-Hebbian LTP in lamina I spinoparabrachial neurons. ***A***, ***B***, Representative primary afferent-evoked EPSCs recorded in projection neurons perfused with normal aCSF (black) or a modified aCSF lacking external Mg^{2+} (gray) when using an intracellular solution supplemented with a vehicle control (***A***) or the NMDAR antagonist MK801 (***B***). ***C***, Internal MK801 significantly reduced the area under the Mg^{2+}-sensitive EPSC in projection neurons ($U = 1$; $^{**}p = 0.002$; Mann–Whitney test) suggesting an effective block of postsynaptic NMDARs. ***D***, Although internal MK801 failed to block non-Hebbian LTP in the combined presence of SKF82958 and dorsal root stimulation, this plasticity was blocked by either addition of the Ca^{2+} chelator BAPTA to the patch solution or bath perfusion with the selective mGluR5 antagonist MPEP ($F_{(3,29)} = 4.481$, $p = 0.011$, one-way ANOVA; $^{*}p < 0.05$, Dunnett's multiple-comparisons test). ***E***, Blocking ryanodine receptors via either bath application of DANT or the intracellular delivery of RYAN suppressed non-Hebbian LTP driven by D1/D5R activation ($F_{(2,15)} = 5.613$, $p = 0.015$, one-way ANOVA; $^{*}p < 0.05$ compared with vehicle control, Dunnett's post test). ***F***, The joint bath application of the D1/D5R agonist SKF82958 and the mGluR5 agonist CHPG enhanced the amplitude of monosynaptic primary afferent-evoked EPSCs in lamina I projection neurons compared with the administration of either agonist alone ($F_{(2,17)} = 9.402$, $p = 0.002$, one-way ANOVA; $^{**}p < 0.01$, Tukey's multiple-comparisons test).

stimulation. Although neither SKF82958 nor CHPG altered synaptic efficacy when applied in isolation, the combination of SKF82958 and CHPG significantly increased the amplitude of monosynaptic primary afferent-evoked EPSCs ($F_{(2,17)} = 9.402$, $p = 0.002$, one-way ANOVA; $p < 0.01$ compared with SKF only or CHPG only, Tukey's multiple-comparisons test; Fig. 6*F*). These findings further support the notion that cooperation between spinal mGluR5 receptors and D1/D5Rs can strongly modulate the strength of sensory inputs onto ascending projection neurons.

Regulation of synaptic plasticity by D1/D5 receptors varies across neuronal populations in the mouse SDH

Mounting evidence suggests that synaptic plasticity occurs in a cell type-dependent manner in the SDH (Ikeda et al., 2003; H. Y. Kim et al., 2015). This includes spike-timing-dependent plasticity at sensory synapses onto SDH neurons, as highly correlated Pre→Post pairings almost exclusively evoke LTP in lamina I spinoparabrachial neurons (Li and Baccei, 2016) but evoke a mixture of LTP, LTD and no change in synaptic efficacy in GABAergic neurons from *Gad67*-EGFP mice (Li and Baccei, 2019). To determine whether the ability of D1/D5R signaling to drive non-Hebbian plasticity at primary afferent synapses varies across different neuronal subpopulations within the spinal nociceptive circuit, we compared the effects of combining the aforementioned primary afferent stimulation (30 stimuli delivered at 0.2 Hz) with bath application of SKF82958 (10 μM) in the following: (1) lamina I spinoparabrachial neurons, (2) *Gad67*-EGFP neurons, and (3) non-GFP neurons, the majority of which correspond to glutamatergic interneurons (Dougherty et al., 2009; Li et al., 2013) within the same spinal cord slices. Notably, non-Hebbian LTP was more frequently observed in lamina I spinoparabrachial neurons (90%; $n = 10$ neurons sampled) than either adjacent *Gad67*-EGFP neurons (25%; $n = 16$) or putative glutamatergic interneurons (40%; $n = 15$), with both populations of interneurons commonly exhibiting either LTD or no change in synaptic efficacy (Fig. 7*A*). Therefore, the prevalence of non-Hebbian LTP was significantly higher in spinoparabrachial neurons compared with interneurons in the SDH ($p = 0.003$; Fisher's exact test). Overall, the effects of combined primary afferent stimulation and D1/D5R activation on the strength of sensory synapses in the SDH varied significantly as a function of neuronal cell type (Kruskal–Wallis statistic = 13.78, $p = 0.001$; Fig. 7*B*).

Discussion

Our findings demonstrate that spinal D1/D5Rs and mGluR5 jointly govern a switch between Hebbian and non-Hebbian LTP at primary afferent synapses onto lamina I spinoparabrachial neurons. Non-Hebbian plasticity within the dorsal horn has been proposed as a potential mechanism driving secondary hyperalgesia and mechanical allodynia after tissue injury (Naka

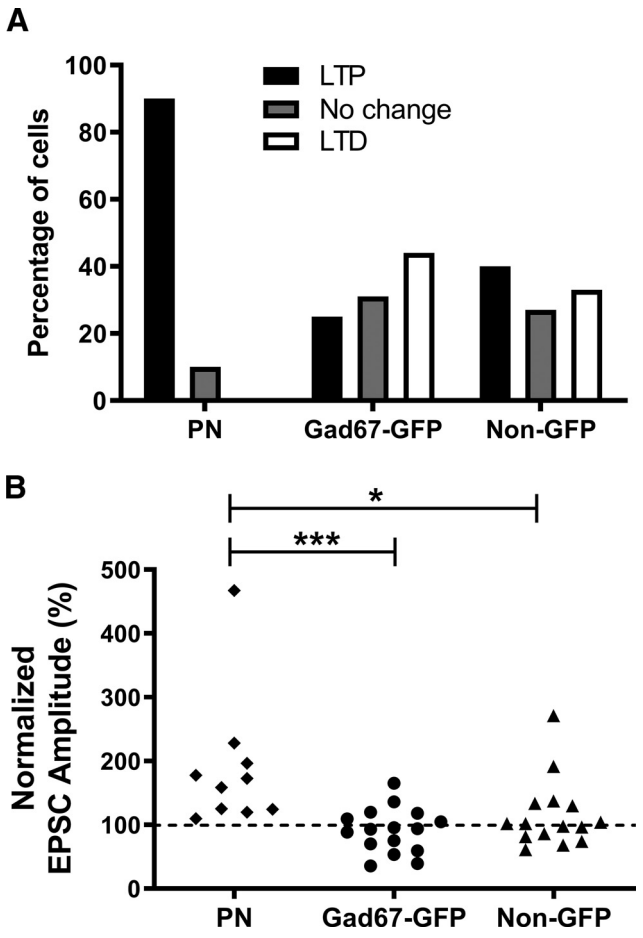

Figure 7. Non-Hebbian LTP enabled by D1/D5R activation is more prevalent in spinoparabrachial neurons than interneurons in the spinal dorsal horn. ***A***, Plot of the percentage of neurons that exhibited LTP in the combined presence of SKF82958 and primary afferent stimulation within the sampled populations of projection neurons (PN), GABAergic interneurons (*Gad67*-GFP), and putative glutamatergic interneurons (Non-GFP). ***B***, The overall magnitude of synaptic potentiation evoked by SKF82958 combined with primary afferent stimulation was significantly greater in lamina I projection neurons compared with GABAergic and presumed glutamatergic interneurons within the same spinal cord slices (Kruskal–Wallis statistic = 13.78, $p = 0.001$; *$p = 0.028$, ***$p = 0.007$, Dunn's multiple-comparisons test).

et al., 2013). Collectively, the available evidence points to the existence of multiple forms of non-Hebbian plasticity within the SDH. Although sustained postsynaptic depolarization of unidentified rat lamina I neurons is sufficient to induce non-Hebbian LTP mediated by L-type voltage-gated Ca^{2+} channels (Naka et al., 2013), the plasticity induced in projection neurons by D1/D5R signaling occurred independently of postsynaptic depolarization and was not observed when the D1/D5R agonist was combined with postsynaptic firing alone (Fig. 4).

D1/D5Rs evoke LTP of C fiber-evoked field potentials in the spinal dorsal horn (Yang et al., 2005; Buesa et al., 2016). However, given that projection neurons represent <5% of all neurons in the region (Spike et al., 2003; Cameron et al., 2015), their activation likely makes a negligible contribution to such extracellular potentials, which predominantly reflect the firing of dorsal horn interneurons. It is difficult to confidently extrapolate findings obtained using field potentials to sensory synapses onto projection neurons in light of the emerging evidence suggesting that the same pattern of electrical stimulation can evoke opposite effects on synaptic efficacy in spinal interneurons versus projection neurons (H. Y. Kim et al., 2015; Li and Baccei, 2019). Indeed, our data show that although D1/D5Rs enable non-Hebbian LTP at sensory synapses onto multiple subpopulations of dorsal horn neurons, this form of plasticity was significantly more prevalent in spinoparabrachial neurons compared with adjacent interneurons (Fig. 7).

It remains unclear if D1/D5R activation must occur concurrently with sensory input to evoke non-Hebbian LTP. Interestingly, activating D1/D5Rs even minutes after the electrical stimulation protocol has been completed can elicit LTP in the hippocampus but only at synapses that were periodically active following the initial pairing protocol (Brzosko et al., 2015). Meanwhile, the activation of β-adrenergic receptors in the prefrontal cortex can favor the subsequent induction of spike-timing-dependent LTP even if the pairing protocol is administered 40–50 min later (Seol et al., 2007; Brzosko et al., 2019). This raises the intriguing, as yet untested, possibility that D1/D5R signaling in the SDH can retroactively and/or proactively potentiate sensory inputs to the spinal nociceptive network. If so, this would suggest that dopamine release in the SDH need not occur simultaneously with the arrival of nociceptive inputs in order for those same inputs to be strengthened. Instead, primary afferent activity could trigger dopamine release via supraspinal loops involving descending pathways originating from the A11 nucleus, which then not only retrospectively potentiates sensory synapses that were recently active but also primes previously inactive synapses to undergo LTP following subsequent noxious stimulation, thereby potentially creating a vicious cycle of synaptic potentiation. Although the A11 nucleus is thought to be the dominant source of spinal dopamine (Skagerberg et al., 1982; Skagerberg and Lindvall, 1985), neurons residing in other brain regions such as the A10 nucleus (Lindvall et al., 1983; Qu et al., 2006) might also contribute to the release of dopamine into the dorsal horn. Furthermore, tyrosine hydroxylase-expressing cells are found in the dorsal root ganglia (DRG; Price and Mudge, 1983; Brumovsky et al., 2006) and dorsal horn (Hou et al., 2016) which could potentially influence dopaminergic tone within spinal nociceptive circuits.

Although the results from D5R knock-out mice strongly implicate D5Rs in the generation of non-Hebbian LTP at primary afferent synapses (Fig. 2), D1Rs are also expressed in the SDH (Megat et al., 2018), and it remains possible that the observed plasticity requires both D5R and D1R activation. D1/D5Rs can regulate synaptic efficacy via the activation of downstream G_s-adenylate cyclase–cAMP/protein kinase A signaling (Otmakhova and Lisman, 1998; Nomura et al., 2014; Rozas et al., 2015). The present study raises the interesting question of whether other G_s-linked receptors may induce similar non-Hebbian LTP at sensory synapses onto spinal projection neurons. Notably, the activation of the EP2 subtype of prostaglandin E_2 receptor also strengthens sensory synapses onto lamina I spinoparabrachial neurons (Li et al., 2018). The reduction of SKF82958-enabled LTP by disrupting G-protein signaling (Fig. 5) or intracellular Ca^{2+} release (Fig. 6*D*,*E*) within projection neurons is consistent with the possibility that the D1/D5Rs that cooperate with mGluR5 to drive non-Hebbian plasticity are located postsynaptically. Nonetheless, both DRG (Xie et al., 1998) and spinal dorsal horn neurons (Zhu et al., 2007) reportedly express all five known subtypes of dopamine receptors, although projection neurons have yet to be specifically examined. The relative importance of presynaptic versus postsynaptic D1/D5Rs could be addressed in future studies via the conditional deletion of these receptors from spinoparabrachial neurons (Ford et al., 2018) or DRG neurons (Kim et al., 2016) using available *Drd5*$^{fl/fl}$ and *Drd1a*$^{fl/fl}$

mice. In addition, a potential role for spinal glia cannot be excluded because they express D1/D5Rs (Zhu et al., 2007) and can promote non-Hebbian LTP in the dorsal horn via the release of neuromodulators such as D-serine, TNFα, and IL1β (Gruber-Schoffnegger et al., 2013; Kronschläger et al., 2016).

Prior studies have elucidated sex-dependent roles of D1/D5Rs in the transition from acute to chronic pain, with global D5R knock-out reducing hyperalgesic priming in males but not females (Megat et al., 2018). Meanwhile, D1/D5R activation similarly enables non-Hebbian LTP in projection neurons from males and females (Fig. 4*B*). Furthermore, the genetic deletion of D5R decreased SKF82958-driven LTP in both males and females, pointing to sex-independent effects of D1/D5R on the plasticity of sensory synapses onto spinal projection neurons. This suggests the possibility that the observed sex differences in the pain behaviors related to hyperalgesic priming may instead reflect the differential activation of other neuronal populations within the spinal nociceptive network, such as GABAergic neurons residing in deeper laminae of the dorsal horn (Megat et al., 2018). Indeed, deep dorsal horn neurons seem to be required for hyperalgesic priming in mice (J. Y. Kim et al., 2015).

Although our data strongly suggest that D1/D5R agonists facilitate LTP at sensory synapses onto spinoparabrachial neurons, it should be noted that D3Rs and D4Rs can dampen primary afferent signaling onto lamina I neurons via a reduction in presynaptic glutamate release (Lu et al., 2018). Therefore, it will ultimately be important to identify the net effects of dopamine released into the SDH on the efficacy of sensory synapses onto projection neurons, which could be addressed using optogenetic stimulation of the descending A11 pathway (Koblinger et al., 2018; Liu et al., 2019). The level of dopamine in the SDH could determine whether the pro-nociceptive effects of D1/D5Rs or the antinociceptive effects of D2-D4Rs dominate as D2Rs possess a higher affinity for dopamine than D1/D5Rs (Richfield et al., 1989; Gerlach et al., 2003). In addition, D2Rs can be degraded following their activation by dopamine, whereas D1Rs are recycled to the plasma membrane (Bartlett et al., 2005). As a result, it has been proposed (Liu et al., 2019) that although low dopamine levels may stimulate D2Rs and inhibit pain, an increased dopaminergic tone in the CNS could eventually favor the activation of D1/D5Rs (Bartlett et al., 2005; Paulus and Trenkwalder, 2006; Dias et al., 2015) and thereby exacerbate pain. Notably, dopamine levels in the dorsal horn can be elevated under pathologic conditions (Gao et al., 2001), which could serve to promote non-Hebbian synaptic plasticity within spinal nociceptive circuits.

Our data point to a key role for D5Rs in the relaxation of the timing rules governing spike-timing-dependent LTP following neonatal tissue damage (Fig. 3), but the underlying circuit mechanisms remain to be elucidated. For example, it is currently unclear if early life injury elevates dopamine release in the mature SDH, which could favor D1/D5R activation and thereby unleash non-Hebbian LTP at sensory synapses onto ascending projection neurons. This issue could be addressed via measures of spinal dopamine release in naive and neonatally injured adult mice using fast-scan cyclic voltammetry (Qiao et al., 2021), HPLC (Takeuchi et al., 2007; Zhao et al., 2007), or the fluorescent imaging of dopamine signaling using the recently developed dLight or GRAB-DA (GPCR-activation-based-dopamine) sensors (Patriarchi et al., 2018; Sun et al., 2018). Indeed, other descending inputs to the dorsal horn are strengthened after neonatal tissue damage, such as those originating from the rostral ventromedial medulla (Zhang et al., 2010; Walker et al., 2015). Alternatively, early life surgical injury could persistently alter spinal dopaminergic tone by modulating the local expression of dopamine transporters (Hou et al., 2016) or dopamine receptor expression within the DRG and/or SDH.

In summary, the current findings demonstrate that the timing rules governing LTP at sensory synapses onto the major output neurons of the SDH network are subject to strong control by spinal D1/D5Rs. A switch from Hebbian to non-Hebbian plasticity, whereby primary afferent activity alone suffices to strengthen their synapses onto spinoparabrachial neurons, could favor the excessive amplification of ascending nociceptive transmission to the brain and thereby promote the generation of chronic pain after peripheral nerve or tissue damage.

References

Bartlett SE, Enquist J, Hopf FW, Lee JH, Gladher F, Kharazia V, Waldhoer M, Mailliard WS, Armstrong R, Bonci A, Whistler JL (2005) Dopamine responsiveness is regulated by targeted sorting of D2 receptors. Proc Natl Acad Sci U S A 102:11521–11526.

Benade V, Nirogi R, Bhyrapuneni G, Daripelli S, Ayyanki G, Irappanavar S, Ponnamaneni R, Manoharan A (2017) Mechanistic evaluation of tapentadol in reducing the pain perception using in-vivo brain and spinal cord microdialysis in rats. Eur J Pharmacol 809:224–230.

Björklund A, Skagerberg G (1979) Evidence for a major spinal cord projection from the diencephalic A11 dopamine cell group in the rat using transmitter-specific fluorescent retrograde tracing. Brain research 177:170–175.

Boyd KN, Mailman RB (2012) Dopamine receptor signaling and current and future antipsychotic drugs. Handb Exp Pharmacol 2012: 53–86.

Brennan TJ, Vandermeulen EP, Gebhart GF (1996) Characterization of a rat model of incisional pain. Pain 64:493–502.

Browne TJ, Smith KM, Gradwell MA, Iredale JA, Dayas CV, Callister RJ, Hughes DI, Graham BA (2021) Spinoparabrachial projection neurons form distinct classes in the mouse dorsal horn. Pain 162:1977–1994.

Brumovsky P, Villar MJ, Hökfelt T (2006) Tyrosine hydroxylase is expressed in a subpopulation of small dorsal root ganglion neurons in the adult mouse. Exp Neurol 200:153–165.

Brzosko Z, Schultz W, Paulsen O (2015) Retroactive modulation of spike timing-dependent plasticity by dopamine. Elife 4:e09685.

Brzosko Z, Mierau SB, Paulsen O (2019) Neuromodulation of spike-timing-dependent plasticity: past, present, and future. Neuron 103:563–581.

Buesa I, Aira Z, Azkue JJ (2016) Regulation of nociceptive plasticity threshold and DARPP-32 phosphorylation in spinal dorsal horn neurons by convergent dopamine and glutamate inputs. PloS One 11:e0162416.

Cameron D, Polgár E, Gutierrez-Mecinas M, Gomez-Lima M, Watanabe M, Todd AJ (2015) The organisation of spinoparabrachial neurons in the mouse. Pain 156:2061–2071.

Chisholm KI, Lo Re L, Polgár E, Gutierrez-Mecinas M, Todd AJ, McMahon SB (2021) Encoding of cutaneous stimuli by lamina I projection neurons. Pain 162:2405–2417.

Dias EV, Sartori CR, Marião PR, Vieira AS, Camargo LC, Athie MC, Pagliusi MO, Tambeli CH, Parada CA (2015) Nucleus accumbens dopaminergic neurotransmission switches its modulatory action in chronification of inflammatory hyperalgesia. Eur J Neurosci 42:2380–2389.

Dougherty KJ, Sawchuk MA, Hochman S (2009) Phenotypic diversity and expression of GABAergic inhibitory interneurons during postnatal development in lumbar spinal cord of glutamic acid decarboxylase 67-green fluorescent protein mice. Neuroscience 163:909–919.

Drdla R, Gassner M, Gingl E, Sandkühler J (2009) Induction of synaptic long-term potentiation after opioid withdrawal. Science 325:207–210.

Fleetwood-Walker SM, Hope PJ, Mitchell R (1988) Antinociceptive actions of descending dopaminergic tracts on cat and rat dorsal horn somatosensory neurones. J Physiol 399:335–348.

Ford NC, Ren D, Baccei ML (2018) NALCN channels enhance the intrinsic excitability of spinal projection neurons. Pain 159:1719–1730.

Gao X, Zhang YQ, Zhang LM, Wu GC (2001) Effects of intraplantar injection of carrageenan on central dopamine release. Brain Res Bull 54:391–394.

Gerlach M, Double K, Arzberger T, Leblhuber F, Tatschner T, Riederer P (2003) Dopamine receptor agonists in current clinical use: comparative

dopamine receptor binding profiles defined in the human striatum. J Neural Transm (Vienna) 110:1119–1127.

Gruber-Schoffnegger D, Drdla-Schutting R, Hönigsperger C, Wunderbaldinger G, Gassner M, Sandkühler J (2013) Induction of thermal hyperalgesia and synaptic long-term potentiation in the spinal cord lamina I by TNF-α and IL-1β is mediated by glial cells. J Neurosci 33:6540–6551.

Hansen N, Klein T, Magerl W, Treede RD (2007) Psychophysical evidence for long-term potentiation of C-fiber and Adelta-fiber pathways in humans by analysis of pain descriptors. J of neurophysiology 97:2559–2563.

Hathway GJ, Vega-Avelaira D, Moss A, Ingram R, Fitzgerald M (2009) Brief, low frequency stimulation of rat peripheral C-fibres evokes prolonged microglial-induced central sensitization in adults but not in neonates. Pain 144:110–118.

Hollon TR, Bek MJ, Lachowicz JE, Ariano MA, Mezey E, Ramachandran R, Wersinger SR, Soares-da-Silva P, Liu ZF, Grinberg A, Drago J, Young WS, 3rd, Westphal H, Jose PA, Sibley DR (2002) Mice lacking D5 dopamine receptors have increased sympathetic tone and are hypertensive. J Neurosci 22:10801–10810.

Holmes A, Hollon TR, Gleason TC, Liu Z, Dreiling J, Sibley DR, Crawley JN (2001) Behavioral characterization of dopamine D5 receptor null mutant mice. Behav Neurosci115:1129–1144.

Hou S, Carson DM, Wu D, Klaw MC, Houlé JD, Tom VJ (2016) Dopamine is produced in the rat spinal cord and regulates micturition reflex after spinal cord injury. Exp Neurol 285:136–146.

Ikeda H, Heinke B, Ruscheweyh R, Sandkühler J (2003) Synaptic plasticity in spinal lamina I projection neurons that mediate hyperalgesia. Science 299:1237–1240.

Ikeda H, Stark J, Fischer H, Wagner M, Drdla R, Jäger T, Sandkühler J (2006) Synaptic amplifier of inflammatory pain in the spinal dorsal horn. Science 312:1659–1662.

Jung SJ, Kim SJ, Park YK, Oh SB, Cho K, Kim J (2006) Group I mGluR regulates the polarity of spike-timing dependent plasticity in substantia gelatinosa neurons. Biochem Biophys Res Commun 347:509–516.

Kim HY, Jun J, Wang J, Bittar A, Chung K, Chung JM (2015) Induction of long-term potentiation and long-term depression is cell-type specific in the spinal cord. Pain 156:618–625.

Kim JY, Tillu DV, Quinn TL, Mejia GL, Shy A, Asiedu MN, Murad E, Schumann AP, Totsch SK, Sorge RE, Mantyh PW, Dussor G, Price TJ (2015) Spinal dopaminergic projections control the transition to pathological pain plasticity via a D1/D5-mediated mechanism. J Neurosci 35:6307–6317.

Kim YS, Anderson M, Park K, Zheng Q, Agarwal A, Gong C, Saijilafu Young L, He S, LaVinka PC, Zhou F, Bergles D, Hanani M, Guan Y, Spray DC, Dong X (2016) Coupled activation of primary sensory neurons contributes to chronic pain. Neuron 91:1085–1096.

Klein T, Magerl W, Hopf HC, Sandkühler J, Treede RD (2004) Perceptual correlates of nociceptive long-term potentiation and long-term depression in humans. J Neurosci 24:964–971.

Koblinger K, Füzesi T, Ejdrygiewicz J, Krajacic A, Bains JS, Whelan PJ (2014) Characterization of A11 neurons projecting to the spinal cord of mice. PloS One 9:e109636.

Koblinger K, Jean-Xavier C, Sharma S, Füzesi T, Young L, Eaton SEA, Kwok CHT, Bains JS, Whelan PJ (2018) Optogenetic activation of A11 region increases motor activity. Front Neural Circuits 12:86.

Kronschläger MT, Drdla-Schutting R, Gassner M, Honsek SD, Teuchmann HL, Sandkühler J (2016) Gliogenic LTP spreads widely in nociceptive pathways. Science 354:1144–1148.

Lang S, Klein T, Magerl W, Treede RD (2007) Modality-specific sensory changes in humans after the induction of long-term potentiation (LTP) in cutaneous nociceptive pathways. Pain 128:254–263.

Li J, Blankenship ML, Baccei ML (2013) Deficits in glycinergic inhibition within adult spinal nociceptive circuits after neonatal tissue damage. Pain 154:1129–1139.

Li J, Baccei ML (2016) Neonatal tissue damage promotes spike timing-dependent synaptic long-term potentiation in adult spinal projection neurons. J Neurosci 36:5405–5416.

Li J, Serafin E, Baccei ML (2018) Prostaglandin signaling governs spike timing-dependent plasticity at sensory synapses onto mouse spinal projection neurons. J Neurosci 38:6628–6639.

Li J, Baccei ML (2019) Neonatal injury alters sensory input and synaptic plasticity in GABAergic interneurons of the adult mouse dorsal horn. J Neurosci 39:7815–7825.

Lindvall O, Björklund A, Skagerberg G (1983) Dopamine-containing neurons in the spinal cord: anatomy and some functional aspects. Ann Neurol 14:255–260.

Liu S, Tang Y, Shu H, Tatum D, Bai Q, Crawford J, Xing Y, Lobo MK, Bellinger L, Kramer P, Tao F (2019) Dopamine receptor D2, but not D1, mediates descending dopaminergic pathway-produced analgesic effect in a trigeminal neuropathic pain mouse model. Pain 160:334–344.

Lu Y, Doroshenko M, Lauzadis J, Kanjiya MP, Rebecchi MJ, Kaczocha M, Puopolo M (2018) Presynaptic inhibition of primary nociceptive signals to dorsal horn lamina I neurons by dopamine. J Neurosci 38:8809–8821.

Megat S, Shiers S, Moy JK, Barragan-Iglesias P, Pradhan G, Seal RP, Dussor G, Price TJ (2018) A critical role for dopamine D5 receptors in pain chronicity in male mice. J Neurosci 38:379–397.

Men DS, Matsui Y (1994) Peripheral nerve stimulation increases serotonin and dopamine metabolites in rat spinal cord. Brain Res Bull 33:625–632.

Naka A, Gruber-Schoffnegger D, Sandkühler J (2013) Non-Hebbian plasticity at C-fiber synapses in rat spinal cord lamina I neurons. Pain 154:1333–1342.

Nomura S, Bouhadana M, Morel C, Faure P, Cauli B, Lambolez B, Hepp R (2014) Noradrenalin and dopamine receptors both control cAMP-PKA signaling throughout the cerebral cortex. Front Cell Neurosci 8:247.

Oliva AA Jr, Jiang M, Lam T, Smith KL, Swann JW (2000) Novel hippocampal interneuronal subtypes identified using transgenic mice that express green fluorescent protein in GABAergic interneurons. J Neurosci 20:3354–3368.

Otmakhova NA, Lisman JE (1998) D1/D5 dopamine receptors inhibit depotentiation at CA1 synapses via cAMP-dependent mechanism. J Neurosci 18:1270–1279.

Patriarchi T, Cho JR, Merten K, Howe MW, Marley A, Xiong WH, Folk RW, Broussard GJ, Liang R, Jang MJ, Zhong H, Dombeck D, von Zastrow M, Nimmerjahn A, Gradinaru V, Williams JT, Tian L (2018) Ultrafast neuronal imaging of dopamine dynamics with designed genetically encoded sensors. Science 360:eaat4422.

Paulus W, Trenkwalder C (2006) Less is more: pathophysiology of dopaminergic-therapy-related augmentation in restless legs syndrome. Lancet Neurol 5:878–886.

Paxinos G, Franklin KB (2012) Paxinos and Franklin's the mouse brain in stereotaxic coordinates. London: Academic Press.

Pfau DB, Klein T, Putzer D, Pogatzki-Zahn EM, Treede RD, Magerl W (2011) Analysis of hyperalgesia time courses in humans after painful electrical high-frequency stimulation identifies a possible transition from early to late LTP-like pain plasticity. Pain 152:1532–1539.

Price J, Mudge AW (1983) A subpopulation of rat dorsal root ganglion neurones is catecholaminergic. Nature 301:241–243.

Qiao Y, Brodnik ZD, Zhao S, Trueblood CT, Li Z, Tom VJ, España RA, Hou S (2021) Spinal dopaminergic mechanisms regulating the micturition reflex in male rats with complete spinal cord injury. J Neurotrauma 38:803–817.

Qu S, Ondo WG, Zhang X, Xie WJ, Pan TH, Le WD (2006) Projections of diencephalic dopamine neurons into the spinal cord in mice. Exp Brain Res 168:152–156.

Richfield EK, Penney JB, Young AB (1989) Anatomical and affinity state comparisons between dopamine D1 and D2 receptors in the rat central nervous system. Neuroscience 30:767–777.

Rozas C, Carvallo C, Contreras D, Carreño M, Ugarte G, Delgado R, Zeise ML, Morales B (2015) Methylphenidate amplifies long-term potentiation in rat hippocampus CA1 area involving the insertion of AMPA receptors by activation of β-adrenergic and D1/D5 receptors. Neuropharmacology 99:15–27.

Ruscheweyh R, Wilder-Smith O, Drdla R, Liu XG, Sandkühler J (2011) Long-term potentiation in spinal nociceptive pathways as a novel target for pain therapy. Mol Pain 7:20.

Sandkühler J, Liu X (1998) Induction of long-term potentiation at spinal synapses by noxious stimulation or nerve injury. Eur J Neurosci 10:2476–2480.

Seol GH, Ziburkus J, Huang S, Song L, Kim IT, Takamiya K, Huganir RL, Lee HK, Kirkwood A (2007) Neuromodulators control the polarity of spike-timing-dependent synaptic plasticity. Neuron 55:919–929.

Skagerberg G, Lindvall O (1985) Organization of diencephalic dopamine neurones projecting to the spinal cord in the rat. Brain Res 342:340–351.
Skagerberg G, Björklund A, Lindvall O, Schmidt RH (1982) Origin and termination of the diencephalo-spinal dopamine system in the rat. Brain Res Bull 9:237–244.
Spike RC, Puskár Z, Andrew D, Todd AJ (2003) A quantitative and morphological study of projection neurons in lamina I of the rat lumbar spinal cord. Eur J Neurosci 18:2433–2448.
Sun F, Zeng J, Jing M, Zhou J, Feng J, Owen SF, Luo Y, Li F, Wang H, Yamaguchi T, Yong Z, Gao Y, Peng W, Wang L, Zhang S, Du J, Lin D, Xu M, Kreitzer AC, Cui G, Li Y (2018) A genetically encoded fluorescent sensor enables rapid and specific detection of dopamine in flies, fish, and mice. Cell 174:481–496.e19.
Taepavarapruk N, Taepavarapruk P, John J, Lai YY, Siegel JM, Phillips AG, McErlane SA, Soja PJ (2008) State-dependent changes in glutamate, glycine, GABA, and dopamine levels in cat lumbar spinal cord. J Neurophysiol 100:598–608.
Takeuchi Y, Takasu K, Honda M, Ono H, Tanabe M (2007) Neurochemical evidence that supraspinally administered gabapentin activates the descending noradrenergic system after peripheral nerve injury. Eur J Pharmacol 556:69–74.
Taniguchi W, Nakatsuka T, Miyazaki N, Yamada H, Takeda D, Fujita T, Kumamoto E, Yoshida M (2011) In vivo patch-clamp analysis of dopaminergic antinociceptive actions on substantia gelatinosa neurons in the spinal cord. Pain 152:95–105.
Walker SM, Fitzgerald M, Hathway GJ (2015) Surgical injury in the neonatal rat alters the adult pattern of descending modulation from the rostroventral medulla. Anesthesiology 122:1391–1400.
Wei H, Viisanen H, Pertovaara A (2009) Descending modulation of neuropathic hypersensitivity by dopamine D2 receptors in or adjacent to the hypothalamic A11 cell group. Pharmacol Res 59:355–363.
Xie GX, Jones K, Peroutka SJ, Palmer PP (1998) Detection of mRNAs and alternatively spliced transcripts of dopamine receptors in rat peripheral sensory and sympathetic ganglia. Brain Res 785:129–135.
Yang HW, Zhou LJ, Hu NW, Xin WJ, Liu XG (2005) Activation of spinal d1/d5 receptors induces late-phase LTP of C-fiber-evoked field potentials in rat spinal dorsal horn. J Neurophysiol 94:961–967.
Zhang HM, Zhou LJ, Hu XD, Hu NW, Zhang T, Liu XG (2004) Acute nerve injury induces long-term potentiation of C-fiber evoked field potentials in spinal dorsal horn of intact rat. Sheng Li Xue Bao 56:591–596.
Zhang JC, Lau PM, Bi GQ (2009) Gain in sensitivity and loss in temporal contrast of STDP by dopaminergic modulation at hippocampal synapses. Proc Natl Acad Sci U S A 106:13028–13033.
Zhang XC, Zhang YQ, Zhao ZQ (2005) Involvement of nitric oxide in long-term potentiation of spinal nociceptive responses in rats. Neuroreport 16:1197–1201.
Zhang YH, Wang XM, Ennis M (2010) Effects of neonatal inflammation on descending modulation from the rostroventromedial medulla. Brain Res Bull 83:16–22.
Zhao H, Zhu W, Pan T, Xie W, Zhang A, Ondo WG, Le W (2007) Spinal cord dopamine receptor expression and function in mice with 6-OHDA lesion of the A11 nucleus and dietary iron deprivation. J Neurosci Res 85:1065–1076.
Zhou LJ, Ren WJ, Zhong Y, Yang T, Wei XH, Xin WJ, Liu CC, Zhou LH, Li YY, Liu XG (2010) Limited BDNF contributes to the failure of injury to skin afferents to produce a neuropathic pain condition. Pain 148:148–157.
Zhu H, Clemens S, Sawchuk M, Hochman S (2007) Expression and distribution of all dopamine receptor subtypes (D(1)-D(5)) in the mouse lumbar spinal cord: a real-time polymerase chain reaction and non-autoradiographic in situ hybridization study. Neuroscience 149:885–897.